Fish & Shellfish Immunology 32 (2012) 513–523

Contents lists available at SciVerse ScienceDirect

Fish & Shellfish Immunology

journal homepage: www.elsevier.com/locate/fsi

Mitochondrial thioredoxin-2 from Manila clam (*Ruditapes philippinarum*) is a potent antioxidant enzyme involved in antibacterial response

Navaneethaiyer Umasuthan [a], Kasthuri Saranya Revathy [a], Youngdeuk Lee [a], Ilson Whang [a], Jehee Lee [a,b,*]

[a] Department of Marine Life Sciences, School of Marine Biomedical Sciences, Jeju National University, Jeju Special Self-Governing Province 690-756, Republic of Korea
[b] Marine and Environmental Institute, Jeju National University, Jeju Special Self-Governing Province 690-814, Republic of Korea

ARTICLE INFO

Article history:
Received 10 August 2011
Received in revised form
24 December 2011
Accepted 26 December 2011
Available online 8 January 2012

Keywords:
Thioredoxin-2
Mitochondria
Antioxidant capacity
Manila clam
Bacterial challenge

ABSTRACT

Thioredoxin (TRx) is a ubiquitous protein involved in the regulation of multiple biological processes. The TRx-2 isoform is exclusively expressed in mitochondria, where it contributes to mitochondrial redox state maintenance. In the present study, a novel thioredoxin-2 gene was identified in the Manila clam, *Ruditapes philippinarum*. The full-length sequence of *RpTRx-2* (1561 bp) consists of a 498 bp coding region encoding a 166 amino acid protein. The N-terminal region of RpTRx-2 harbors a mitochondrial localization signal (56 amino acids), while the C-terminal portion contains the characteristic ^{89}WCGPC^{93} catalytic active site. Phylogenetic analysis revealed that RpTRx-2 is closest to its ortholog from abalone. The broad distribution pattern of *RpTRx-2* mRNA in healthy animal tissues implicates a generally significant function in normal clam physiology. The transcription level of *RpTRx-2*, however, is highest in hemocytes. Lipopolysaccharide and *Vibrio tapetis* bacterium caused up-regulation of the RpTrx-2 transcript levels in gill and hemocytes. Interestingly, clam manganese superoxide dismutase (*MnSOD*) mRNA levels in hemocytes elicited a corresponding response to these immune challenges. RpTRx-2 was recombinantly expressed in *Escherichia coli* BL21 (DE3) and used in insulin disulfide reduction assay as well as metal-catalyzed oxidation assay to elucidate its antioxidant property by reducing substrate and protecting super-coiled DNA from oxidative damage through free radical scavenging, respectively. Collectively, our data indicated that RpTRx-2, a mitochondrial TRx-2 family member, is an antioxidant enzyme that may be involved in antibacterial defense of clams.

1. Introduction

The evolutionarily ancient and simple organisms, such as mollusks, rely solely on the innate arm of the immune response to defend against invading microbes. Yet, the innate immune system is remarkably robust and dynamic enough that it remains a vital component of complex organisms, such as humans, who have evolved the adaptive arm of the immune response as a secondary line of defense. The innate response involves hemocyte-mediated phagocytosis, well known to be a major defense mechanism in invertebrates [1]. Phagocytotic uptake of foreign material stimulates mitochondrial generation of reactive oxygen species (ROS) [2], which are byproducts of molecular O_2 metabolization in aerobic life and may be cytotoxic at elevated levels [3]. Low concentrations of ROS are, however, beneficial in mediating various physiological processes [4], including acting as a hemocyte-mediated antimicrobial defense in bivalves [5]. Thus, the organism must maintain a balance between elevated ROS levels to clear pathogenic infection and reduced levels to protect against detrimental oxidative stress. Biological systems have evolved to maintain such redox homeostasis and include several antioxidant systems comprising enzymatic and non-enzymatic strategies [6]. Intracellular redox regulation depends mainly on glutathione (GSH) and thioredoxin (TRx) buffering systems [7,8]. The TRx antioxidant system, in particular, functions as a catalytic cycle in which peroxiredoxin (PRx) oxidizes the TRx and then TRx reductase (TRxR) reduces it using NADPH [9].

TRx (EC 1.8.4.8) is a 12 kDa multifunctional protein, ubiquitous in all forms of life and exists as either a cytosolic (TRx-1) or mitochondrial (TRx-2) isoform [10]. Catalytic activity of TRx reduces disulfide bridge of substrate via the vicinal Cys residues in its active motif of WCGPC. Apart from its antioxidant-redox regulatory role, TRx is also involved in regulation of growth [11], transcription

* Corresponding author. Marine Molecular Genetics Lab, Department of Marine Life Science, College of Ocean Sciences, Jeju National University, 66 Jejudaehakno, Ara-Dong, Jeju, Jeju-Do 690-756, Republic of Korea. Tel.: +82 64 754 3472; fax: +82 64 756 3493.
E-mail address: jehee@jejunu.ac.kr (J. Lee).

1050-4648/$ – see front matter © 2011 Elsevier Ltd. All rights reserved.
doi:10.1016/j.fsi.2011.12.010

factors [12], protein folding [13] and scavenging radicals [14]. Although many cytosolic thioredoxins have been characterized [15,16], including the RpTRx from *Ruditapes philippinarum* Manila clam [17] that we reported recently, only a few mitochondrial TRx-2s have been described, namely those from rat [18], human [19], chicken [20] and abalone [21].

To gain insight into the role of TRx isoforms in the immunity of the Manila clam, we cloned the full-length cDNA of *TRx-2* from *R. philippinarum*. This species is an important fishery bivalve with high economic value and in recent decades has suffered severe epidemics of infections with various pathogens. In this study, we characterized the newly discovered *RpTRx-2*, determining its basal tissue distribution and transcriptional responses to challenge with LPS and *Vibrio tapetis* bacterium. Using a recombinant protein, the biological activity and antioxidant property of RpTRx-2 were confirmed. Collectively, our data lay a foundation to understand the roles of RpTRx-2 against mitochondrial homeostasis and antibacterial defense in clam.

2. Materials and methods

2.1. Manila clam cDNA library and identification of RpTRx-2

We have established a normalized clam (*R. philippinarum*) cDNA library using RNA isolated from multiple tissues of healthy clams. The basic procedure of cDNA library construction, normalization and initial GS-FLX™ sequencing strategies has been described in our previous report [17]. BLAST analysis (http://blast.ncbi.nlm.nih.gov/Blast) of the clam cDNA shotgun sequence database identified a putative cDNA with high homology to known *TRx-2* members, designated as Manila clam *TRx-2* (*RpTRx-2*) and further characterized.

2.2. In silico characterization of RpTRx-2

The full-length nucleotide and amino acid sequence of RpTRx-2 was analyzed using the NCBI BLAST program and TRx-2 homologs were retrieved. DNAssist (2.2) was used to determine the open reading frame (ORF) and encoded amino acid sequence of RpTRx-2, which was further examined using ExPASy proteomics server. The conserved domain (CD) was determined by using prosite profile analysis [22], motif scan Pfam hidden Markov models (HMMs) (Local models) (http://hits.isb-sib.ch/cgi-bin/PFSCAN), and the CD-Database (CDD) protein annotation resource (http://www.ncbi.nlm.nih.gov/Structure/cdd/cdd.shtml). The mitochondrial localization signal (MLS) was deduced by using the MitoProt II Server (v1.101) (http://www.cbs.dtu.dk/services/TargetP/) [23]. Disulfide connectivity was predicted using the DiANNA server [24]. Identity and similarity percentages between RpTRx-2 and orthologues were calculated utilizing EMBOSS pairwise alignment algorithms (http://www.ebi.ac.uk/Tools/emboss/align/). The amino acid sequence of RpTRx-2 was submitted to I-TASSER server [25] to generate a 3D model, based on multiple-threading alignments with potential templates including *Rhodobacter capsulatus* TRx-2 (PDB no, 2pptA) and human TRx-2 (PDB no, 1w4vA) and the predicted model was analyzed by RasMol 2.7.5.2 [26]. Pair-wise and multiple sequence alignments were generated using the ClustalW, version 2.0 [27]. To deduce the phylogenetic relationship, known TRx-2 and TRx-1 sequences were aligned in ClustalW and then the neighbor-joining (NJ) method was applied to construct a phylogenetic tree with 1000 bootstrap replicates using the MEGA 5 program [28].

2.3. Clams, immune challenges and tissue isolation

Clams with an average size of 35 ± 5 mm were collected from the eastern coastal area of Jeju Island (Republic of Korea) and maintained in 80 L tanks of aerated sand-filtered seawater with 34 ± 1‰ salinity and at 21 ± 1 °C. Clams were acclimatized to laboratory conditions for seven days prior to experiment.

In order to evaluate the tissue specific distribution of the *RpTRx-2* mRNA, tissues from adductor muscle, mantle, siphon, gill and foot were isolated from three healthy, unchallenged individuals. Hemolymph (1–2 mL/clam) was also collected from each animal using a sterile syringe; hemocytes were immediately harvested from the biological fluid by centrifugation at 3000 × *g* for 10 min at 4 °C. In order to determine the immune response of *RpTRx-2*, two *in vivo* challenges were devised using lipopolysaccharide (LPS) and intact Gram-negative bacteria *V. tapetis*. LPS and *V. tapetis* were suspended in phosphate buffered saline (PBS). Two groups of clams were randomly chosen for intramuscular (i.m.) injection of either 100 μL LPS (50 ng/μL, *Escherichia coli* 055:B5; Sigma–Aldrich, USA) or 100 μL of *V. tapetis* (1.9×10^9 cells/mL). A third group of uninjected clams was used as control.

Hemocyte and gill samples were collected at 3, 6, 12, 24, 48, and 96 h post-injection (p.i.) from at least three clams of the LPS-, bacterial-injected and control groups. Tissues and hemocytes were snap frozen in liquid nitrogen and stored at −80 °C until processing for RNA extraction.

2.4. Total RNA isolation and cDNA synthesis

The total RNA was extracted from 50 mg of tissue sample and hemocyte samples using the Tri Reagent™ (Sigma–Aldrich). Purified RNA concentration was determined by measuring the absorbance at 260 nm in a UV-spectrophotometer (Bio-Rad). The total RNA was stored at −80 °C until further use.

RNA samples were thawed and diluted to 1 μg/μL concentration and used as template in cDNA synthesis using PrimeScript™ first-strand cDNA synthesis kit (Takara). The cDNA synthesis reaction was carried out according to the manufacturer's instructions. The synthesized cDNA product was diluted appropriately and used in quantitative real-time PCR (qRT-PCR).

2.5. RpTRx-2 transcriptional profiling by qRT-PCR

The *RpTRx-2* mRNA expression profile was determined by qRT-PCR, along with that for the gene of manganese superoxide dismutase (MnSOD) *RpMnSOD*. *RpTRx-2* gene-specific primers (F1, 5′-GTCCTTGTAAGCTGTTAGGGCCAA-3′ and R1, 5′-ATCACATCGTCGTCT TGAAGCCCT-3′) generated a 199 bp fragment of *RpTRx-2*. The *RpMnSOD* gene-specific primers (F, 5′-AAGGACATGTTGACACAG GCTTCG-3′ and R, 5′-AAAGCCTGTTGTTGGTTGCAGAGG-3′) generated a 135 bp fragment of *RpMnSOD*. The gene coding for clam *β-actin* was amplified by using *Rp-β-actin* gene-specific primers (F, 5′-CTCCCTTGAGAAGAGCTACGA-3′ and R, 5′-GATACCAGCAGAT TCCATACCC-3′) and used as an invariant control [29]. Tissue-specific distribution of *RpTRx-2* was determined by measuring mRNA expression levels in adductor muscle, mantle, siphon, gill, foot and hemocytes. Pathogen inducibility was demonstrated in hemocytes and gill by using a time course experiment. qRT-PCR assays were performed in 20 μL reaction system containing 4 μL of diluted cDNA from different tissues, 10 μL of 2× Takara SYBR premix Ex *Taq*™, 0.8 μL of each primer (10 pmol/μL), and 5 μL dH_2O. A Thermal Cycler Dice™ Real-Time System (Takara) was used with the following cycling profile: a single denaturation cycle of 95 °C for 10 s; 45 amplification cycles of 95 °C for 5 s, 58 °C for 10 s, and 72 °C for 20 s; and a final single cycle of 95 °C for 15 s, 60 °C for 30 s, and 95 °C for 15 s. The relative *RpTRx-2* mRNA expression was determined by the Livak $2^{-\Delta\Delta CT}$ method [30], using the clam *β-actin* as a reference gene. To quantify the tissue-specific expression, the expression level of *RpTRx-2* in adductor muscle was used as the

calibrator, to which the expression levels in all other tissues were compared. To determine the fold-change in expression induced by challenges with purified toxin or bacteria, the expressional level of tissues from injected animals were compared with those from uninjected controls.

2.6. Cloning of RpTRx-2 coding region

Two *RpTRx-2* gene-specific primers (F2, 5′-GAGAGAgaattcAT GGCATCTAGAGCAATATTACGTAGAGTGGT-3′ and R2, 5′-GAGAGA ctgcagTTAACCAATTAATTTGTCTAGAAACGTTTCAATCACATCGTC-3′) harboring restriction sites for *Eco*RI and *Pst*I, respectively (underlined), were used to amplify the coding region of *RpTRx-2*, which was then cloned into the pMAL-c2X expression vector. Amplification was carried out in a 50 μL reaction system containing 5 μL of 10× Ex *Taq* buffer, 5 U of Ex *Taq* polymerase (Takara), 8 μL of 2.5 mM dNTPs, 40 pmol of each primer, and 50 ng of cDNA from hemocyte. The PCR cycling profile was as follows: a single denaturation step of 94 °C for 3 min; 30 amplification cycles of 94 °C for 30 s, 58 °C for 30 s, and 72 °C for 45 s; and a final extension step of 72 °C for 5 min. Products were purified using the Accuprep® PCR purification kit (Bioneer Co.), and digested along with the maltose binding protein (MBP)-fused expression vector (pMAL-c2X) using the corresponding restriction enzymes. After electrophoretic resolution on a 1% agarose gel, the desired fragments were excised and purified using the Accuprep® gel purification kit (Bioneer Co.). The digested *RpTRx-2* coding sequence and vector were ligated by overnight incubation with T4 DNA ligase (Takara) at 16 °C. The recombinant construct pMAL-c2X/*RpTRx-2* was then transformed into *E. coli* DH5α cells, purified and sequenced (Macrogen).

2.7. Recombinant RpTRx-2 (rRpTRx-2) expression and purification

The confirmed recombinant pMAL-c2X/*RpTRx-2* construct was transformed into *E. coli* BL21 (DE3) cells (Novagen) to overexpress the rRpTRx-2. A 100 mL aliquot of starter culture was inoculated into 900 mL of rich medium (Luria broth, 1 mg/mL amphicillin and 0.2% glucose) and grown at 37 °C with shaking at 150 rpm until the optical density reached 0.6 at 600 nm. Cells at log phase were induced by 0.5 mM of isopropyl-β-thiogalactopyranoside (IPTG) at 37 °C for 2 h, and then harvested by centrifugation at 3500 rpm for 30 min at 4 °C. The cell pellet was resuspended in column buffer (20 mM Tris–HCl, pH 7.4, 200 mM NaCl) and lysozyme was added at a final concentration of 1 mg/mL and the mixture was incubated for 1 h on ice. Then, cells were subjected to cold sonication and lysate was centrifuged at 9000 × *g* for 30 min at 4 °C. The crude extract containing the MBP-tagged rRpTRx-2 was collected and purified using the pMAL protein-fusion and purification technique [31]. Purified samples collected from different steps were analyzed on 12% SDS-PAGE along with standard molecular mass marker (Takara). The concentration of the purified rRpTRx-2 was determined by the Bradford method [32]. The purified MBP-tagged rRpTRx-2 was used in subsequent assays.

2.8. Functional characterization of rRpTRx-2

2.8.1. Insulin disulfide reduction assay

The enzymatic activity of rRpTRx-2 was assayed based on its ability to reduce insulin, as previously described [33], but with slight modifications. In brief, the reaction was carried out in a 500 μL system, containing 100 mM potassium phosphate buffer (pH 7.0), 2 mM EDTA, 130 μM insulin from bovine pancreas (Sigma–Aldrich), 0.6 mM dithiothretol (DTT; USB, Amersham Life Sciences) and purified rRpTRx-2. The reaction was initiated by addition of insulin to the system and then allowed to occur for 10 min at 25 °C. The insolubilization of reduced-insulin was monitored at 650 nm. A non-enzymatic reduction of insulin by DTT was concurrently monitored in a solution in which RpTRx-2 was absent. Under the same conditions, an assay using MBP was performed to determine the effect of the MPB-tag protein. One unit of enzyme activity was defined as the required amount of enzyme that increased the absorbance by 1.0 at 650 nm under the above-described conditions.

2.8.2. Metal-catalyzed oxidation (MCO) protection assay

The potential of rRpTRx-2 to protect super-coiled DNA against DTT/Fe^{3+}/O_2 mediated damage was assessed using an *in vitro* MCO assay, as described in previous reports [34,35]. In brief, 100 μL reaction systems containing 1.65 mM DTT, 16.5 μM $FeCl_3$ and different concentrations of rRpTRx-2 (from 6.25 to 200 ng/μL) were pre-incubated at 37 °C for 2.5 h. Then, 1 μg of pUC19 super-coiled DNA was added to each system prior to incubation at 37 °C for an additional 2.5 h. Subsequently, reaction components were purified using a PCR purification system (Bioneer Co.) and DNA degradation was evaluated by electrophoresis on a 1% agarose gel. Corresponding concentrations of MBP and bovine serum albumin (BSA) were concurrently assayed as controls, under the same conditions.

2.9. Statistical analysis

All the results are reported as mean ± standard deviation (SD) of triplicates. Intergroup differences were analyzed by one-way analysis of variance (ANOVA) followed by Duncan's multiple-range test using the SPSS statistical software package (version 11.5; SPSS, Inc.). Statistical significance was set at $P < 0.05$.

3. Results

3.1. Structural characterization of RpTRx-2

3.1.1. Sequence characterization of RpTRx-2

In the present study, a complete cDNA sequence (contig 18326) was identified from our Manila clam cDNA library, based upon its high homology with previously reported TRx-2 family members. The cDNA was designated as *R. philippinarum* thioredoxin-2 (RpTRx-2) and the sequence data were deposited in GenBank under accession no. JF499394. Nucleotide and amino acid sequences of RpTRx-2 are shown in Fig. 1. The cDNA of *RpTRx-2* was 1561 bp long, and consisted of a 5′-untranslated region (UTR) of 149 bp and a 3′-UTR of 914 bp. The 3′-UTR harbored three RNA instability motifs (ATTTA), located at 1087–1091, 1203–1207 and 1386–1390 bp. An open reading frame (ORF) of 498 bp encoded a polypeptide of 166 amino acids with an estimated molecular mass of 18,719 Da and a predicted pI of 9.08. The MotifScan program identified a thioredoxin domain in the 60–164 amino acid region, and the prosite program indicated a potential thioredoxin family element located from ^{82}Val to ^{100}Leu that overlapped with the redox-active site of ^{89}WCGPC^{93}. MitoProt II Server predicted a 56 amino acid long MLS (score: 0.9985) which was predicted to commence with an α-helix and continue with two subsequent β-sheets (Fig. 1). Therefore, RpTRx-2 was demonstrated to have two main regions of its N-terminal segment with high content of positively charged residues and the C-terminal region which is comparable to classical cytosolic TRx (Figs. 1 and 2). Disulfide connectivity analysis showed that RpTRx-2 contained four Cys residues that were responsible for forming two disulfide bonds at ^{52}C–^{93}C and ^{90}C–^{125}C. RpTRx-2 also harbored an invariant proline residue at position 78. There was no evidence for either signal peptide or N-glycosylation sites in RpTRx-2.

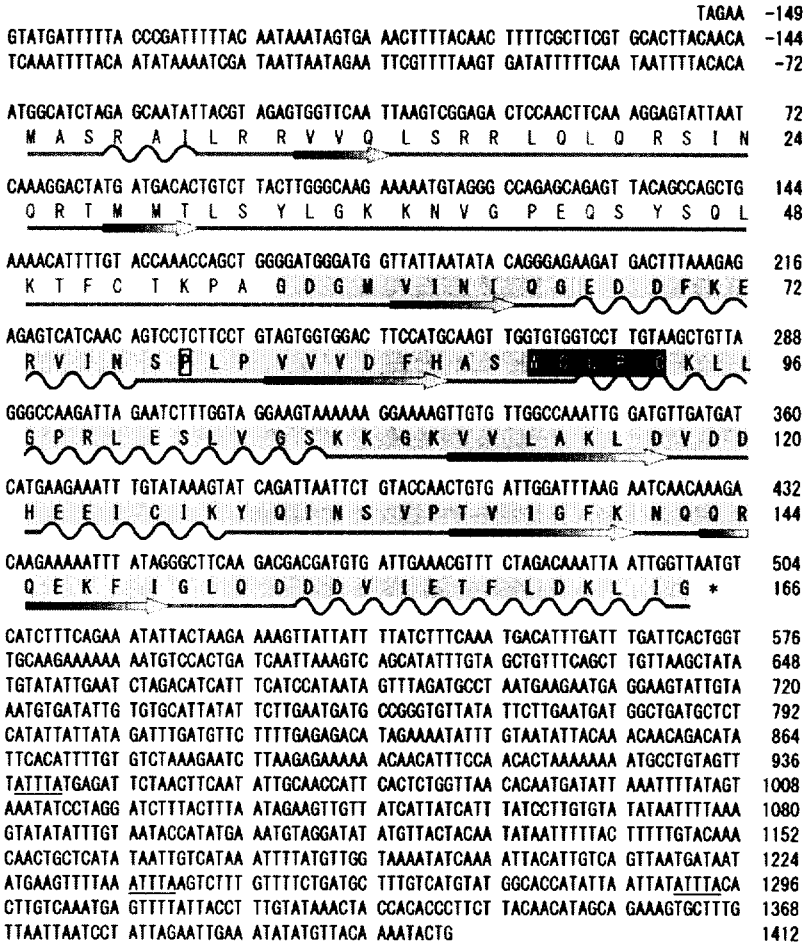

Fig. 1. The cDNA (black), deduced amino acid (blue) sequences and secondary structure of *R. philippinarum* TRx-2 (GenBank accession no. JF499394). Stop (TAA) codon is denoted with an asterisk. The mature peptide (cytosolic counterpart) is contrasted from predicted N-terminal mitochondrial localization signal by gray shading. The invariant proline residue is boxed. The active site motif ^{89}WCGPC^{93} is shaded in black. The RNA instability motifs (ATTTA) are underlined. Secondary structural components are shown below the amino acid sequence: blue line, coil; red wave, α-helix; green arrow, β-sheet. (For interpretation of the references to color in this figure legend, the reader is referred to the web version of this article.)

3.1.2. Tertiary structural modeling of RpTRx-2

Using multiple TRx protein templates, the potential tertiary structure of RpTRx-2 was constructed. The 3D structure of RpTRx-2 was composed of a five β-strands primary core surrounded by four α-helixes and an extended N-terminal fold (Fig. 2A). Cys residues of active motif were located, one at the end of a β-sheet (C^{90}) and other one at the beginning of an α-helix (C^{93}). Interestingly, the potential structure of cytosolic homolog, RpTRx (Fig. 2B) was comparable to that of C-terminal cytosolic domain of RpTRx-2 (Fig. 2C).

3.1.3. Homology analysis and multiple alignments of RpTRx-2

The results of pairwise alignments demonstrated that RpTRx-2 shared 24.5–44.8 (%) identity and 44.5–63.4 (%) similarity to all the other known TRx-2 sequences. Interestingly, RpTRx-2 shared highest homology with the cattle TRx-2 homolog (Table 1). Moreover, the previously identified Manila clam cytosolic thioredoxin (RpTRx) [17] shared only 36% of similarity with RpTRx-2. Multiple alignment analysis using RpTRx-2 (§ in Fig. 3) and various other lineages revealed that RpTRx-2 consisted of two unique domains: an N-terminal MLS region and a C-terminal cytosolic counterpart (Figs. 2A and 3). The TRx family active site motif WCGPC and common flanking residues were highly conserved in RpTRx-2. It was interesting to note that invertebrate (molluskan) TRx-2s demonstrated significant variation from that of vertebrate sequences, especially in the sequences where the vertebrate sequences are most tightly conserved.

3.1.4. Phylogenetic characterization of RpTRx-2

Based on an alignment using deduced amino acid sequences of 40 thioredoxin orthologues from various lineages, we constructed a phylogenetic tree. The tree was rooted with two bacterial thioredoxins, *E. coli* DH1 TRx-2 (BAJ44365) and *E. coli* TRx-1 (AAA24534). Two main families formed branches from the origin of out groups, those being mitochondrial thiredoxins (TRx-2) and cytosolic thiredoxins (TRx-1). In TRx-2 family, molluskan TRx-2 formed a distinct branch where RpTRx-2 (●) was placed closer to abalone TRx-2. On the other hand, Manila clam TRx-1 (RpTRx: ●) was positioned together with TRx-1 from Japanese scallop (Fig. 4). Thus, our results demonstrated that RpTRx-2 and RpTRx belong to distinct subfamilies of thioredoxins and were derived from a common ancestor.

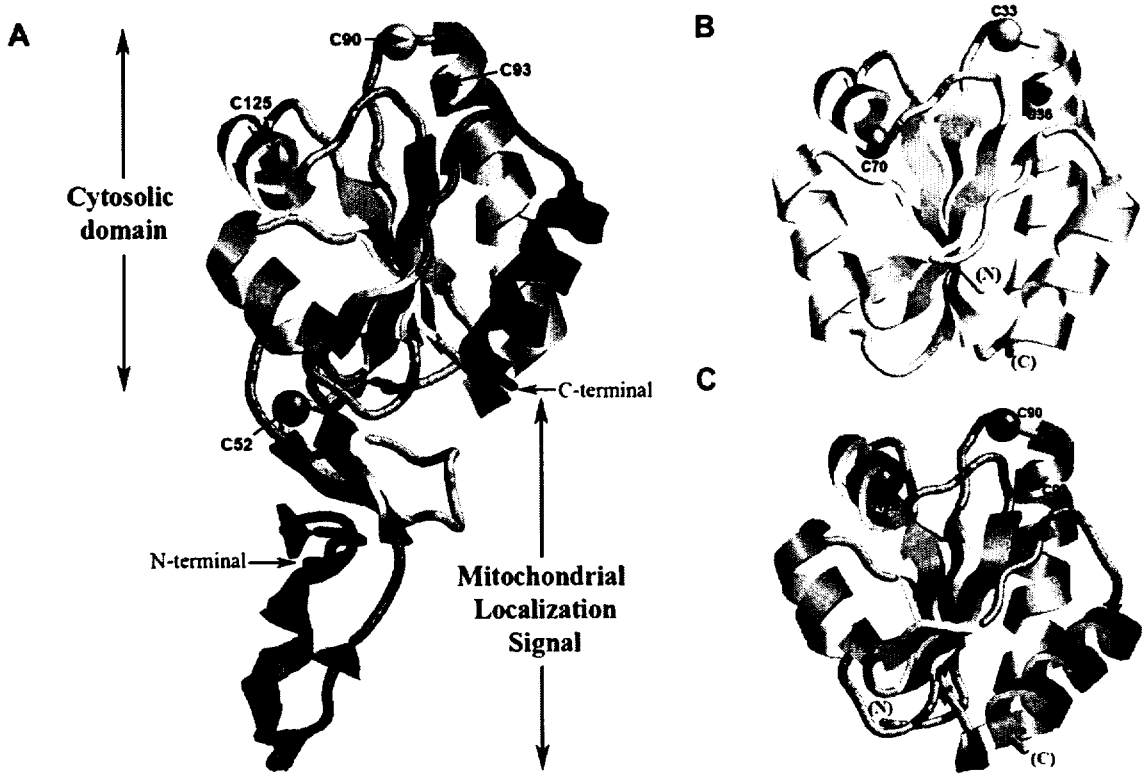

Fig. 2. Predicted 3D structure of RpTRx-2 and comparison of C-terminal domain of RpTRx-2 with RpTRx. Ribbon diagrams of (A) complete RpTRx-2 showing its two domain folding and four Cys residues, (B) homologous RpTRx and its Cys residues and (C) C-terminal cytosolic counterpart of RpTRx-2.

3.2. Transcriptional characterization of RpTRx-2

3.2.1. Tissue-specific expression of RpTRx-2

In order to determine the differential tissue-specific mRNA expression profile of *RpTRx-2*, qRT-PCR was performed using gene-specific primers targeting its coding region. Clam *β-actin* was used as an invariant control gene and relative transcription level was further compared with transcription level in adductor muscle. *RpTRx-2* mRNA was constitutively expressed in all tissues examined (Fig. 5), but the levels were significantly higher in mantle, gill and hemocytes. Compared to adductor muscle, the highest mRNA level was detected in hemocytes (51-fold; $P < 0.05$). Expression

Table 1
Identity and similarity (%) of Manila clam TRx-2 to other orthologues.

Common name	Species	Molecular name	Accession No	I (%)	S (%)	G (%)	AA
Cattle	*Bos taurus*	Mitochondrial thioredoxin	NP_776633	44.8	63.4	7.0	166
Disc abalone	*Haliotis discus discus*	Thioredoxin 2	ABO26636	44.5	63.2	13.7	173
Budgerigar	*Melopsittacus undulatus*	Thioredoxin 2	AAO72715	43.1	63.5	13.2	146
Human	*Homo sapiens*	Thioredoxin 2	AAF86467	43.0	59.8	14.5	166
Norway rat	*Rattus norvegicus*	Mitochondrial thioredoxin	NP_445783	41.8	62.1	12.4	166
House mouse	*Mus musculus*	Mitochondrial thioredoxin	NP_064297	41.8	61.6	12.4	166
Chicken	*Gallus gallus*	Mitochondrial thioredoxin	NP_001026581	41.8	56.5	20.0	140
Atlantic salmon	*Salmo salar*	Mitochondrial thioredoxin	ACM09441	41.7	62.3	9.7	167
African clawed frog	*Xenopus laevis*	Thioredoxin 2	AAH43794	41.6	65.3	5.8	170
Western clawed frog	*Xenopus (Silurana) tropicalis*	Thioredoxin 2	NP_001008161	40.1	58.2	15.4	170
Green anole	*Anolis carolinensis*	Mitochondrial thioredoxin-like	XP_003220982	40.0	62.3	7.4	171
Zebrafish	*Danio rerio*	Mitochondrial thioredoxin	NP_991204	37.4	57.2	22.5	166
Domestic silkworm	*Bombyx mori*	Mitochondrial thioredoxin 2	ABD36368	33.3	53.7	22.0	149
Roundworm	*Caenorhabditis elegans*	Thioredoxin 2	NP_505651	33.1	53.6	13.3	144
Mozambique tilapia	*Oreochromis mossambicus*	Thioredoxin 2	AAX61130	31.7	46.7	32.7	167
Leafcutter ant	*Acromyrmex echinatior*	Mitochondrial thioredoxin	EGI58159	30.8	52.1	19.5	139
House mosquito	*Culex quinquefasciatus*	Mitochondrial thioredoxin	XP_001845536	30.8	53.3	20.7	169
Asian tiger mosquito	*Aedes albopictus*	Mitochondrial thioredoxin 2	AAV90706	30.3	53.4	23.6	148
Pig roundworm	*Ascaris suum*	Thioredoxin 2	ADY44298	24.5	44.5	26.4	216
Manila clam	*Venerupis philippinarum*	Thioredoxin 1	JF499393	21.5	36.0	41.9	106

Pair-wise identity percentage was calculated using EMBOSS alignment (http://www.ebi.ac.uk) by maintaining open gap penalty and gap extension penalty levels at 10.0 and 0.5, respectively. I, identity; S, similarity; G, gap; AA, amino acids.

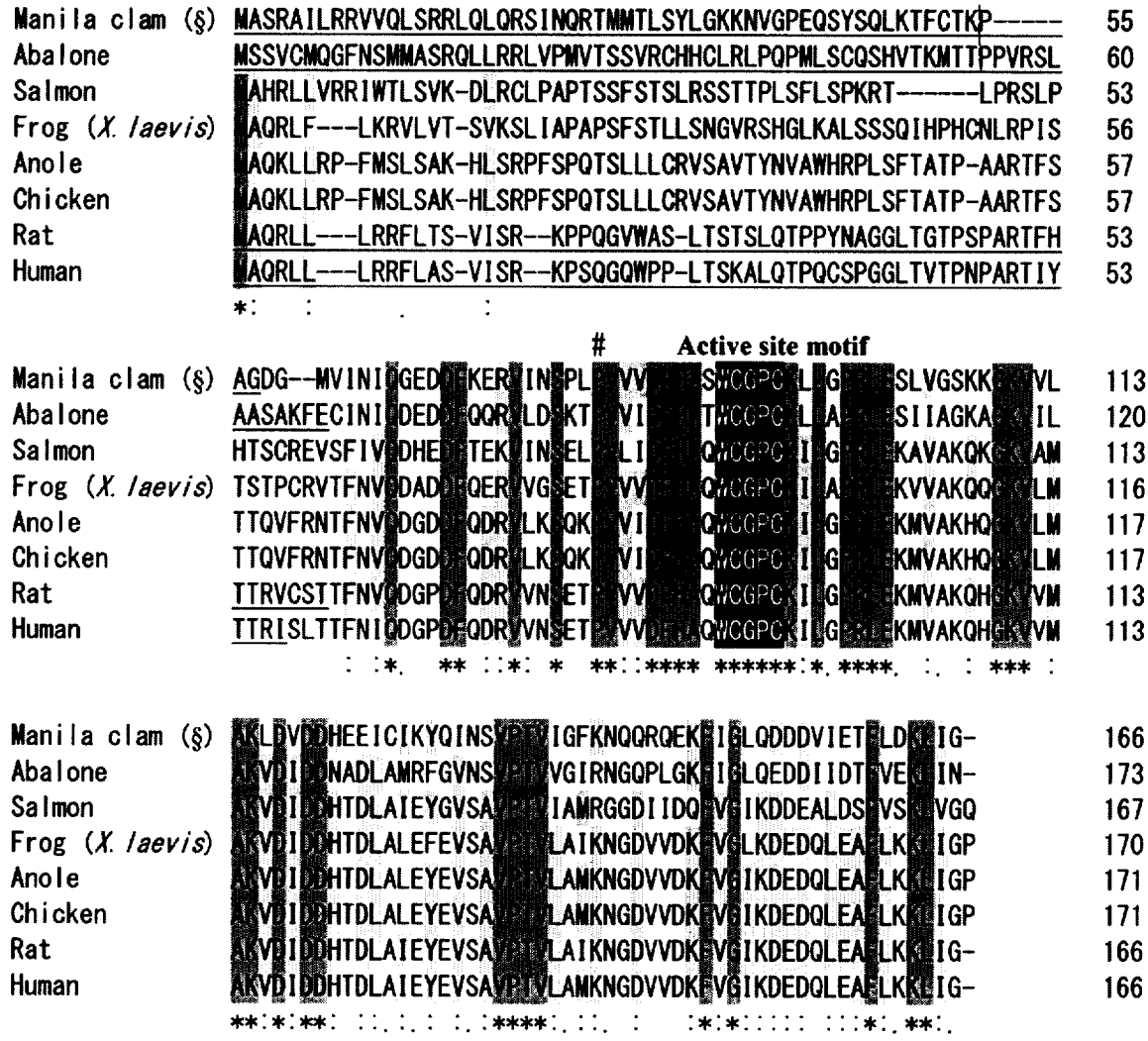

Fig. 3. Multiple alignment of *R. philippinarum* TRx-2 (§) with known homologs. Residues shaded with dark gray (*) and light gray (:) are completely (100%) and strongly conserved, respectively. Weak conservation is marked by (.). The WCGPC active site is shaded in black. Mitochondrial localization signals are underlined, wherever references were available. The invariant proline residue is marked by (#). The accession numbers of TRx-2 orthologues are given in Table 1.

levels of *RpTRx-2* mRNA in siphon, foot and adductor muscle were similar ($P < 0.05$). Thus, *RpTRx-2* transcript showed a tissue-specific expression profile in clam tissues.

3.2.2. Pathogen-modulated RpTRx-2 transcription

We investigated the transcriptional response of *RpTRx-2* in gill and hemocytes to immune challenges, by using LPS endotoxin and a potent Manila clam pathogen *V. tapetis* [36]. *RpTRx-2* was significantly up-regulated in gills of immune-challenged animals ($P < 0.05$), with the highest induced expression (2-fold increases) occurring at 6 h post-LPS challenge and at 24 and 96 h post-bacterial challenge (Fig. 6). Hemocytic transcription level of *RpTRx-2* was found to be most significantly elevated (13.2-fold; $P < 0.05$) at 6 h against LPS-challenge (Fig. 7A). Bacterial challenge also induced increases in hemocytic *RpTRx-2* mRNA levels; the highest level (4.3-fold) was reached at 48 h p.i., as compared to uninjected clams (Fig. 7B). To demonstrate the corresponding induction of superoxide dismutase members, clam *MnSOD* mRNA level was determined at the post-challenge time points, as well. Both immune challenges led to up-regulated MnSOD transcription (post-LPS induction data not shown). Interestingly, the *V. tapetis*-induced transcriptional profile patterns of *RpTRx-2* and *RpMnSOD* were similar, as they both elicited their highest mRNA levels at 48 h (Fig. 7C).

3.3. Recombinant expression and purification of rRpTRx-2

The *RpTRx-2* coding sequence was subcloned into the *malE* gene encoding MBP under the strong tac promoter in the pMAL-c2X expression vector. The recombinant RpTRx-2 was overexpressed using an *in vitro* translating system, *E. coli* BL21 (DE3) cells by IPTG-driven induction. Fractions collected at different stages of affinity chromatography were examined by SDS-PAGE (Fig. 8) and indicated that the molecular mass of the purified fusion rRpTRx-2 was around 61.5 kDa. This finding agreed with our predicted value for molecular mass of putative RpTRx-2 (~19 kDa), since the molecular mass of the MBP-tag was 42.5 kDa. Biological properties of RpTRx-2 were then characterized using the purified rRpTRx-2.

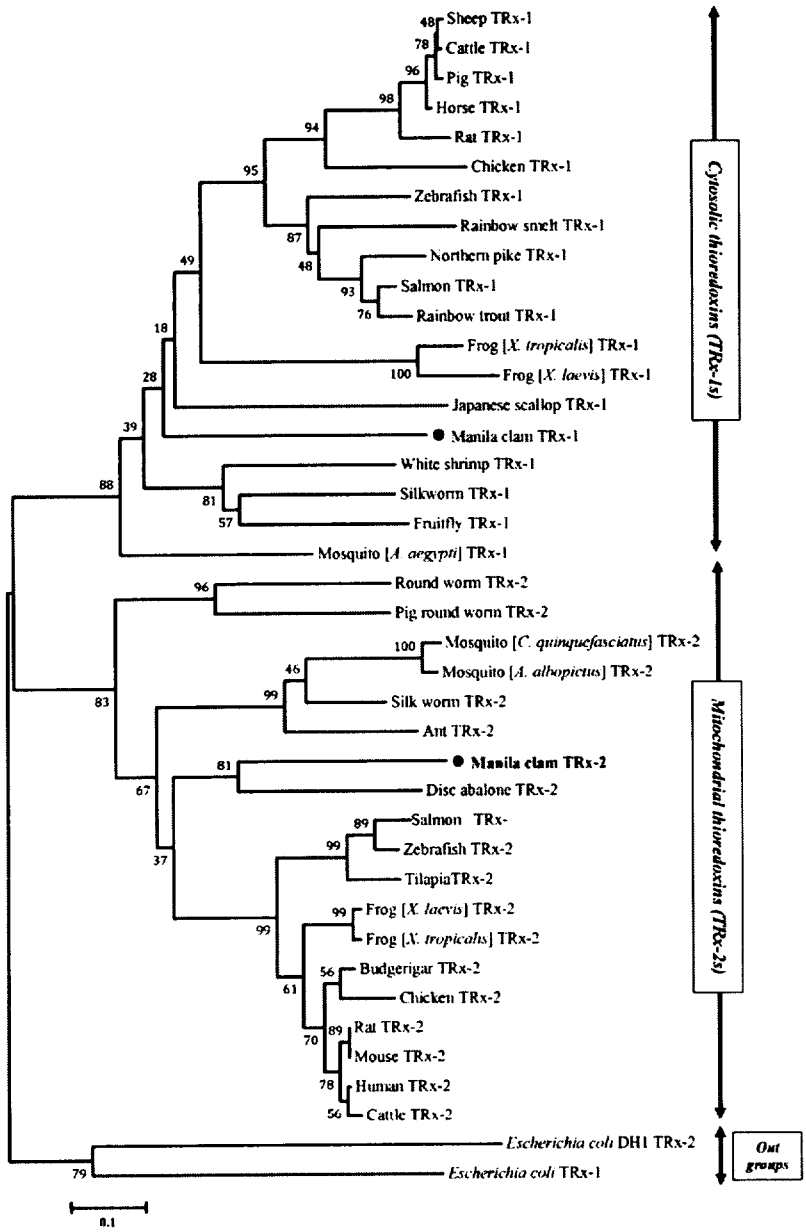

Fig. 4. Phylogenetic analysis of RpTRx-2 (●) and RpTRx-1 (●) with other known thioredoxin protein sequences. The tree was generated by the MEGA 5 program using the NJ method. The tree was rooted with a TRx-2 and a TRx-1 from bacteria, *Escherichia coli* DH1 (BAJ44365) and *Escherichia coli* (AAA24534), respectively. The branches were validated by bootstrap analysis from 1000 replications, which are represented by percentages in branch nodes. TRx-2 protein sequences used in this study are listed in Table 1. Accession numbers for the TRx-1 sequences are as follows: Manila clam *R. philippinarum*, (JF499393); Sheep *Ovis aries*, (NP_001009421); Pig *Sus scrofa*, (NP_999478); Horse *Equus caballus*, (NP_001075282); African clawed frog *Xenopus laevis* (NP_001088487); Western clawed frog *Xenopus (Silurana) tropicalis*, (NP_001011127); Rainbow smelt *Osmerus mordax*, (ACO09971); Northern pike *Esox lucius*, (ACO13599); Atlantic salmon *Salmo salar*, (CM09596); Rainbow trout *Oncorhynchus mykiss*, (ACO08786); Yellow fever mosquito *Aedes aegypti*, (AAK70900); Fruit fly *Drosophila melanogaster*, (AAF37263); Domestic silkworm *Bombyx mori*, (ABM92269); white shrimp *L. vannamei*, (ACA60746); Japanese scallop *Chlamys farreri*, (AAV73827); Cattle *Bos taurus* (NP_776393); Zebrafish *Danio rerio* (NP_001002461); Rat *Rattus norvegicus* (NP_446252); and Chicken *Gallus gallus* (NP_990784).

3.4. Functional characterization of RpTRx-2

3.4.1. Insulin disulfide reduction assay

In order to investigate whether RpTRx-2 is functionally involved in the clam antioxidant system, an *in vitro* turbidimetric assay was used to evaluate the recombinant protein's ability to reduce insulin disulfides mediated by DTT. Fig. 9 shows insulin reduction that was facilitated by the rRpTRx-2. As compared to negative control (with no rRpTRx-2), insulin reduction increased directly in proportion to rRpTRx-2 concentration. The control assay performed with MBP showed that in the absence of rRpTRx-2, there was no significant ($P < 0.05$) change in absorbance at 650 nm. The average specific activity of rRpTRx-2 for the tested dose-range was 3.098 U/mg, where one unit of the insulin reduction enzymatic activity was defined as the amount of enzyme that can change the absorbance by 1.0 at 650 nm under standard reaction conditions (as described in Section 2.8.1).

3.4.2. Protection of DNA from oxidative cleavage

The antioxidant role of rRpTRx-2 was investigated using a DNA nicking assay. Protection of DNA from damage in an MCO system

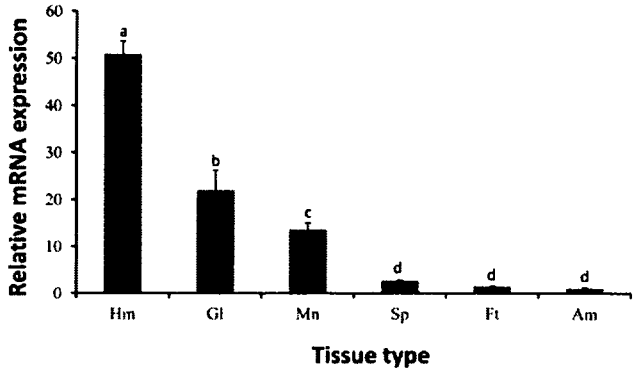

Fig. 5. Tissue-specific differential expression analysis of RpTRx-2 mRNA determined by quantitative real-time PCR. The relative *RpTRx-2* transcript level of each tissue was calculated by the $2^{-\Delta\Delta CT}$ method using Manila clam *β-actin* as reference gene and compared to that from adductor muscle. Tissues: Am, adductor muscle; Ft, foot; Sp, siphon; Mn, mantle; Hm, hemocytes; and Gl, gill. The error bars represent SD of $n = 3$. Data with different letters are significantly different at $P < 0.05$.

was assessed, in which the MCO system generates 'OH radicals that can damage the DNA [37] and consequently converts DNA from super-coiled form to nicked form. The extent of DNA damage was indicated by distinct mobility shift patterns produced by the two DNA forms after electrophoretic resolution on a gel (Fig. 10). When rRpTRx-2 was absent, DNA underwent maximum damage in the MCO system (lane e). Addition of rRpTRx-2 to the MCO system effectively diminished the DNA nicking caused by radicals (lanes g–l) in a dose-dependent manner. Maximum protection of super-coiled DNA from damage (~75%) was observed with the 200 ng/μL of rRpTRx-2.

4. Discussion

The mitochondrion is the major physiological source of ROS generation during oxidative metabolism [14]. Thus, these organelles have evolved a quenching system to internally regulate redox homeostasis; the mitochondrion antioxidant network consists of TRx-2, TRxR and PRx. Prior to our study presented herein, only one molluskan TRx-2 had been cloned [21], while multiple isoforms of TRx had been identified in other organisms, ranging from the simple *E. coli* [38] and yeast [39] to the complex rat [18] and human

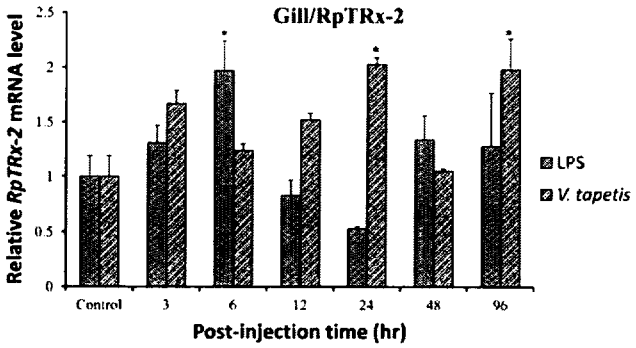

Fig. 6. Expression profile of *RpTRx-2* mRNA in clam gill after LPS and *V. tapetis* challenges, as determined by SYBR green RT-PCR. The relative expression was calculated by the $2^{-\Delta\Delta CT}$ method using Manila clam *β-actin* as reference gene and compared to that from uninjected control. The error bars represent SD of $n = 3$. Data with same symbols are at the same level of significance at $P < 0.05$.

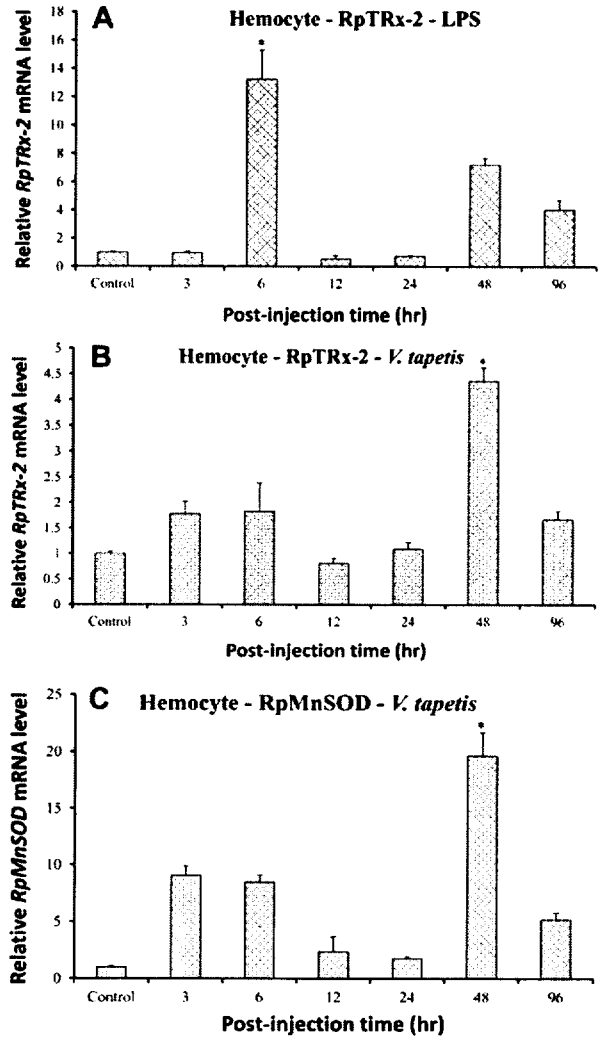

Fig. 7. Expression profiles of *RpTRx-2* mRNA in clam hemocytes after (A) LPS and (B) *V. tapetis* challenges, and that of *RpMnSOD* mRNA in hemocytes after (C) *V. tapetis* challenge, as determined by SYBR green RT-PCR. The relative expression was calculated by the $2^{-\Delta\Delta CT}$ method using Manila clam *β-actin* as reference gene and compared to uninjected control. The error bars represent SD of $n = 3$. Data with different symbols are significantly different at $P < 0.05$, among the different time points.

[19]. Thus, the identification, cloning, and characterization of the cDNA encoding RpTRx-2 from *R. philippinarum* enhances our overall knowledge of this particular enzyme family.

4.1. Sequence characterization

The putative RpTRx-2 isoform features several characteristics that have been defined for TRx family members. All TRx members consist of a canonical WCGPC motif within a highly conserved fold. The Cys residues found in WCGPC motif represent the catalytic center by which the reduction of disulfide bridges in substrates is carried out. This motif was located in RpTRx-2 within a TRx family element (Fig. 1). The mitochondrial TRx isoform harbors a unique N-terminal peptide that distinguishes it from the cytosolic TRx isoform and facilitates translocation into the mitochondria. Accordingly, RpTRx-2 comprised a two domain structure, having an N-terminal MLS (*pI*: 11.8) and a C-terminal region (*pI*: 4.9) that is homologous to cytosolic thioredoxin (RpTRx) (Fig. 2). The characteristic features of MLS in

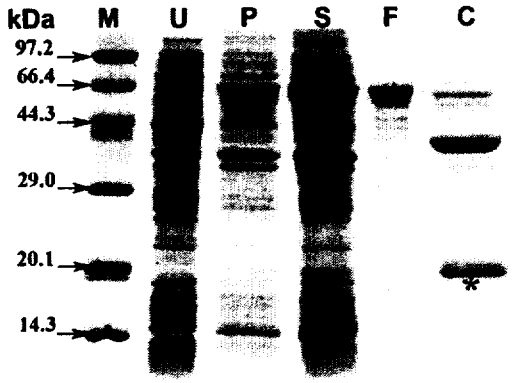

Fig. 8. SDS-PAGE analysis of overexpressed and purified recombinant RpTRx-2 protein in fusion and cleaved forms. Lanes: M, molecular mass marker (sizes are indicated in kilodaltons); U, total cellular extract from *E. coli* BL21 (DE3) before IPTG induction; P, insoluble fraction of proteins after IPTG-induction; S, soluble fraction of proteins after IPTG-induction; F, purified recombinant fusion protein rRpTRx-2/MBP; C, rRpTRx-2 (*) cleaved from MBP-tag using factor Xa.

mitochondrial proteins, including the presence of basic motifs, have been extensively studied [40,41]. RpTRx-2 harbors an MLS enriched in positively charged residues, such as Arg (12%), Ser (10%) and Leu (12%). Moreover, deduced secondary structure of RpTRx-2 (Fig. 1) and attributes of its MLS were similar to rat TRx-2 [18]. The molecular masses of the mature proteins produced from the TRx-2 isoforms of rat [18], human [42] and abalone [21], after the cleavage at putative mitochondrial peptidase cleavage site, have been reported as 12.2 kDa, 12 kDa and 11.6 kDa, respectively. Similarly, the mature RpTRx-2 isoform was predicted to have a molecular mass of 12.2 kDa. Some of the conserved residues in mammalian TRx-2 isoforms (Phe^{70}, Pro^{80}, Pro^{98} and Asp^{117}) were also found to be conserved in RpTRx-2. Sequence analysis of RpTRx-2 showed that it shared significant identity with TRx-2 homologs, as compared to other TRx-1 isoforms, including RpTRx [17]. In addition, RpTRx-2 tertiary structure was consistent with the canonical α/β thioredoxin fold structure (Fig. 2). Although RpTRx-2 demonstrated relatively higher homology to mammalian TRx-2 members, as opposed to that of lower order vertebrates and invertebrates (Table 1), the phylogenetic analysis clearly established its position within the invertebrate cluster (Fig. 4). Therefore, our data strongly suggest that *R. philippinarum* TRx-2 is a novel member of the growing subfamily of mitochondrial TRx proteins.

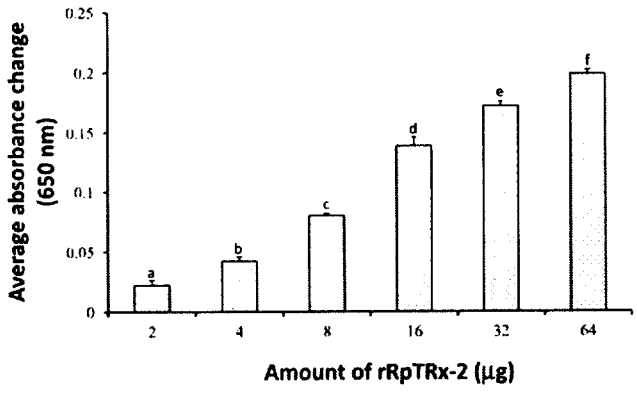

Fig. 9. Insulin disulfide reduction by recombinant RpTRx-2. Insulin and DTT were incubated without (negative control) or with different amounts (2–64 μg) of rRpTRx-2. Insulin reducing activity of rRpTRx-2 was spectrophotometrically quantified by measuring absorbance at 650 nm and compared with negative control. Data with different letters are significantly different ($P < 0.05$) among different doses of rRpTRx-2.

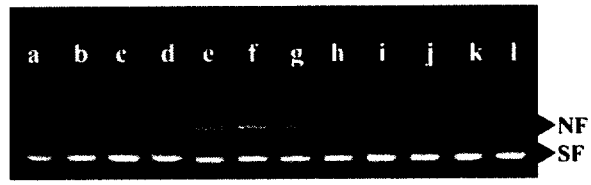

Fig. 10. Potential of recombinant RpTRx-2 to protect super-coiled DNA from cleavage in an MCO system. Lanes: a, pUC19 without any treatment; b, pUC19 incubated with water; c, pUC19 incubated with 1.65 mM DTT only; d, pUC19 incubated with 16.5 μM $FeCl_3$ only; e, pUC19 incubated with MCO system only (16.5 μM $FeCl_3$ and 1.65 mM DTT); f, pUC19 incubated with MCO system and 0.5 mg/mL BSA (control); g–l, pUC19 incubated with MCO system and different concentrations (6.25, 12.5, 25, 50, 100 and 200 ng/μL) of purified rRpTRx-2, respectively. NF, nicked form; SF, super-coiled form of pUC19.

4.2. Transcriptional analysis

Reactive oxygen species, including O_2^-, $^{\cdot}OH$ and H_2O_2, are considered to be dual-role players in normal physiology, as they have both beneficial and deleterious impacts on living systems. The cumulative generation of ROS, endo- or exogenously, can cause oxidative stress that may lead to cellular redox imbalance [43,44]. Therefore, antioxidant systems have evolved as crucial mediators to counteract the negative consequences of ROS.

Mammalian *TRx-2*s have been reported as abundantly expressed in tissues with higher metabolic activity, such as heart, kidney, muscle, and liver [18,19]. *RpTRx-2* was constitutively and differentially expressed in all examined tissues in our study (Fig. 5), suggesting its possible functional involvement against oxidative injury of mitochondrion in a broad spectrum of tissues. Particularly, it was most highly transcribed in mantle, gill and hemocytes. Once the skin barriers are breached in bivalves, innate immune responses are stimulated and involve both cellular- and humoral-mediated mechanisms. The cellular immune responses are largely mediated by hemocytes. In a recent review, Donaghy et al. emphasized substantially versatile immune defensive roles played by clam hemocytes [2]. Thus, the observed higher expression of *RpTRx-2* in Manila clam hemocytes and gill may be attributed to their broad functional roles in immunity and defense against pathogens entering by filter feeding (environmental exposure) or O_2 transport function, respectively.

Few studies in the literature have focused on TRx expression profiling in response to various pathophysiological stimulants. Abalone *TRx-2* has been shown to be up-regulated in response to H_2O_2-induced oxidative stress [21]. Moreover, pathogen-induced stimulation of thioredoxin was reported against virus in *Fenneropenaeus chinensis* shrimp [45] and against bacteria in *Eriocheir sinensis* crab [46] and *R. philippinarum* [17]. *RpTRx-2* mRNA was likewise induced by LPS and *V. tapetis* in gill and hemocytes, and this induction corresponded with up-regulated mRNA levels of another antioxidant enzyme, RpMnSOD (Fig. 7). The response of increased *RpTRx-2* transcriptional activity in hemocytes was more robust than in gill. LPS-induced hemocytic *RpTRx-2* transcription was comparable to that of *Listonella anguillarum*-induced expression of *EsTRx-1* [46] and white spot syndrome virus-challenged expression of *FcTRx* [45]. *V. tapetis* challenge led to up-regulated transcription of *RpTRx-2*, *RpMnSOD* and cytosolic *RpTRx* [17] at 48 h p.i. The MnSOD antioxidant enzyme is functionally related to the TRxs and associated with redox balance. A previous report has shown that *MnSOD* expression increased in parallel to that of *TRx-2* under hypoxic conditions [47]. *MnSOD* has also been reported to be involved in transient systemic immune responses in *F. chinensis* [48] against viral challenge, and in *Argopecten irradians* [49] against bacterial challenge. Microbial-induced phagocytosis is associated with elevated production of ROS [50]. Hence, our results support

the hypothesis that the TRx system, in conjunction with SOD members, may play a protective role against microbial-induced ROS generation during phagocytosis.

4.3. Functional characterization

In order to address the biological activity of the rRpTRx-2 described in this study, we performed a classical assay of insulin disulfide bridge-reduction in the presence of DTT. A crustacean TRx from *Litopenaeus vannamei* showed specific activity of 10.44 $\Delta A_{650\ nm}$/mg [51]. Likewise, rRpTRx-2 dose-dependently reduced the insulin with a specific activity of 3.098 U/mg. This value is comparable to that reported for abalone TRx-2 (1.83) [21], *E. coli* TRx (4.93) and calf liver TRx (5.09) [33], suggesting that RpTRx-2 has dithiol-reducing enzymatic activity.

High levels of ROS cause damage to all types of biological macromolecules, especially, to DNA [43]. The ROS generating MCO system was employed in this study to demonstrate the ability of rRpTRx-2 to protect super-coiled DNA from nicking. Results indicated that rRpTRx-2 (at 200 ng/μL) effectively protected more than 75% of super-coiled DNA from damage (Fig. 10), suggesting a scavenging capacity that is similar to that of its cytosolic homolog [17]. In addition, the DNA-protection against oxidative damage by thioredoxin also has been demonstrated in abalone (TRx-2) [21] and sweet potato (TRx-h) [52]. Chicken TRx-2 was previously shown to regulate the mitochondrial apoptosis signaling pathway by scavenging ROS, and suppression of TRx-2 expression enhanced ROS accumulation and lead to apoptosis [20]. Human TRx-2 has also been suggested to play a defensive role against oxidative damage and oxidant-induced cell death [19]. Similarly, our data suggested that RpTRx-2 may act as a component of the clam mitochondrial antioxidant system, scavenging and clearing free radicals in order to establish intra-mitochondrion homeostasis. However, other physiological and defense related roles of the mitochondrion antioxidant system have yet to be fully elucidated and it is possible that RpTRx-2 contributes significantly to those.

5. Conclusion

In summary, a mitochondrial TRx-2 was identified from *R. philippinarum*, Manila clam. A recombinant rRpTRx-2 was generated and used to demonstrate the antioxidant protective activities of this enzyme. *RpTRx-2* was found to be constitutively expressed throughout Manila clam tissues, but was most highly expressed in the immune-related tissues, gill and hemocytes. LPS- and *V. tapetis*-challenges stimulated *RpTRx-2* transcription, in conjunction with increased *RpMnSOD* mRNA. Thus, we have discovered a novel TRx-2 member with antioxidant property, which could contribute to the antibacterial defense mechanisms in Manila clam.

Acknowledgment

This research was supported by the Marine and Extreme Genome Research Center Program of the Ministry of Land, Transportation and Maritime Affairs and by the Basic Science Research Program through the National Research Foundation of Korea (NRF) funded by the Ministry of Education, Science and Technology (2010-0014481).

References

[1] Reade PC. Phagocytosis in invertebrates [ast]. Australian Journal of Experimental Biology and Medical Science 1968;46:219–29.
[2] Donaghy L, Lambert C, Choi K-S, Soudant P. Hemocytes of the carpet shell clam (*Ruditapes decussatus*) and the Manila clam (*Ruditapes philippinarum*): current knowledge and future prospects. Aquaculture 2009;297:10–24.
[3] Kanzok SM, Fechner A, Bauer H, Ulschmid JK, Müller H-M, Botella-Munoz J, et al. Substitution of the thioredoxin system for glutathione reductase in *Drosophila melanogaster*. Science 2001;291:643–6.
[4] MatÉs JM, Pérez-Gómez C, De Castro IN. Antioxidant enzymes and human diseases. Clinical Biochemistry 1999;32:595–603.
[5] Anderson RS. Hemocyte-derived reactive oxygen intermediate production in four bivalve mollusks. Developmental & Comparative Immunology 1994;18:89–96.
[6] Halliwell B. Antioxidants in human health and disease. Annual Review of Nutrition 1996;16:33–50.
[7] McEligot AJ, Yang S, Meyskens J, Frank L. Redox regulation by intrinsic species and extrinsic nutrients in normal and cancer cells. Annual Review of Nutrition 2005;25:261–95.
[8] Moriarty-Craige SE, Jones DP. Extracellular thiols and thiol/disulfide redox in metabolism. Annual Review of Nutrition 2004;24:481–509.
[9] Kalinina EV, Chernov NN, Saprin AN. Involvement of thio-, peroxi-, and glutaredoxins in cellular redox-dependent processes. Biochemistry Biokhimiia 2008;73:1493–510.
[10] Holmgren A. Thioredoxin. Annual Review of Biochemistry 1985;54:237–71.
[11] Rubartelli A, Bonifaci N, Sitia R. High rates of thioredoxin secretion correlate with growth arrest in hepatoma cells. Cancer Research 1995;55:675–80.
[12] Matthews JR, Wakasugi N, Virelizier JL, Yodoi J, Hay RT. Thioredoxin regulates the DNA binding activity of NF-kappa B by reduction of a disulphide bond involving cysteine 62. Nucleic Acids Research 1992;20:3821–30.
[13] Berndt C, Lillig CH, Holmgren A. Thioredoxins and glutaredoxins as facilitators of protein folding. Biochimica et Biophysica Acta 2008;1783:641–50.
[14] Schallreuter KU, Wood JM. The role of thioredoxin reductase in the reduction of free radicals at the surface of the epidermis. Biochemical and Biophysical Research Communications 1986;136:630–7.
[15] Wahl MC, Irmler A, Hecker B, Schirmer RH, Becker K. Comparative structural analysis of oxidized and reduced thioredoxin from *Drosophila melanogaster*. Journal of Molecular Biology 2005;345:1119–30.
[16] Powis G, Montfort WR. Properties and biological activities of thioredoxins. Annual Review of Pharmacology and Toxicology 2001;41:261–95.
[17] Revathy KS, Umasuthan N, Lee Y, Whang I, Kim HC, Lee J. Cytosolic thioredoxin from *Ruditapes philippinarum*: molecular cloning, characterization, expression and DNA protection activity of the recombinant protein. Developmental & Comparative Immunology; 2011.
[18] Spyrou G, Enmark E, Miranda-Vizuete A, Gustafsson J-Å. Cloning and expression of a novel mammalian thioredoxin. Journal of Biological Chemistry 1997;272:2936–41.
[19] Chen Y, Cai J, Murphy TJ, Jones DP. Overexpressed human mitochondrial thioredoxin confers resistance to oxidant-induced apoptosis in human osteosarcoma cells. Journal of Biological Chemistry 2002;277:33242–8.
[20] Tanaka T, Hosoi F, Yamaguchi-Iwai Y, Nakamura H, Masutani H, Ueda S, et al. Thioredoxin-2 (TRX-2) is an essential gene regulating mitochondria-dependent apoptosis. The EMBO Journal 2002;21:1695–703.
[21] De Zoysa M, Pushpamali WA, Whang I, Kim SJ, Lee J. Mitochondrial thioredoxin-2 from disk abalone (*Haliotis discus discus*): molecular characterization, tissue expression and DNA protection activity of its recombinant protein. Comparative Biochemistry and Physiology Part B: Biochemistry and Molecular Biology 2008;149:630–9.
[22] Bairoch A, Bucher P, Hofmann K. The PROSITE database, its status in 1997. Nucleic Acids Research 1997;25:217–21.
[23] Claros MG, Vincens P. Computational method to predict mitochondrially imported proteins and their targeting sequences. European Journal of Biochemistry 1996;241:779–86.
[24] Ferre F, Clote P. DiANNA: a web server for disulfide connectivity prediction. Nucleic Acids Research 2005;33:W230–2.
[25] Roy A, Kucukural A, Zhang Y. I-TASSER: a unified platform for automated protein structure and function prediction. Nature Protocols 2010;5:725–38.
[26] Sayle RA, Milner-White EJ. RASMOL: biomolecular graphics for all. Trends in Biochemical Sciences 1995;20:374.
[27] Thompson JD, Higgins DG, Gibson TJ. CLUSTAL W: improving the sensitivity of progressive multiple sequence alignment through sequence weighting, position-specific gap penalties and weight matrix choice. Nucleic Acids Research 1994;22:4673–80.
[28] Kumar S, Tamura K, Nei M. MEGA3: integrated software for molecular evolutionary genetics analysis and sequence alignment. Brief Bioinformatics 2004;5:150–63.
[29] Zhang L, Zhao J, Li C, Su X, Chen A, Li T, et al. Cloning and characterization of allograft inflammatory factor-1 (AIF-1) from Manila clam *Venerupis philippinarum*. Fish & Shellfish Immunology 2011;30:148–53.
[30] Livak KJ, Schmittgen TD. Analysis of relative gene expression data using real-time quantitative PCR and the 2(-Delta Delta C(T)) Method. Methods 2001;25:402–8.
[31] Maina CV, Riggs PD, Grandea 3rd AG, Slatko BE, Moran LS, Tagliamonte JA, et al. An *Escherichia coli* vector to express and purify foreign proteins by fusion to and separation from maltose-binding protein. Gene 1988;74:365–73.
[32] Bradford MM. A rapid and sensitive method for the quantitation of microgram quantities of protein utilizing the principle of protein-dye binding. Analytical Biochemistry 1976;72:248–54.
[33] Holmgren A. Thioredoxin catalyzes the reduction of insulin disulfides by dithiothreitol and dihydrolipoamide. Journal of Biological Chemistry 1979;254:9627–32.

[34] Li J, Zhang WB, Loukas A, Lin RY, Ito A, Zhang LH, et al. Functional expression and characterization of *Echinococcus granulosus* thioredoxin peroxidase suggests a role in protection against oxidative damage. Gene 2004;326:157–65.
[35] Jiang Q, Yan YH, Hu GK, Zhang YZ. Molecular cloning and characterization of a peroxiredoxin from *Phanerochaete chrysosporium*. Cellular & Molecular Biology Letters 2005;10:659–68.
[36] Paillard C, Korsnes K, Le Chevalier P, Le Boulay C, Harkestad L, Eriksen AG, et al. *Vibrio tapetis*-like strain isolated from introduced Manila clams *Ruditapes philippinarum* showing symptoms of brown ring disease in Norway. Diseases of Aquatic Organisms 2008;81:153–61.
[37] Chae HZ, Chung SJ, Rhee SG. Thioredoxin-dependent peroxide reductase from yeast. Journal of Biological Chemistry 1994;269:27670–8.
[38] Miranda-Vizuete A, Damdimopoulos AE, Gustafsson J, Spyrou G. Cloning, expression, and characterization of a novel *Escherichia coli* thioredoxin. Journal of Biological Chemistry 1997;272:30841–7.
[39] Pedrajas JR, Kosmidou E, Miranda-Vizuete A, Gustafsson JA, Wright AP, Spyrou G. Identification and functional characterization of a novel mitochondrial thioredoxin system in *Saccharomyces cerevisiae*. Journal of Biological Chemistry 1999;274:6366–73.
[40] Hendrick JP, Hodges PE, Rosenberg LE. Survey of amino-terminal proteolytic cleavage sites in mitochondrial precursor proteins: leader peptides cleaved by two matrix proteases share a three-amino acid motif. Proceedings of the National Academy of Sciences 1989;86:4056–60.
[41] Emanuelsson O, von Heijne G. Prediction of organellar targeting signals. Biochimica et Biophysica Acta (BBA) – Molecular Cell Research 2001;1541: 114–9.
[42] Jin J, Chen X, Zhou Y, Bartlam M, Guo Q, Liu Y, et al. Crystal structure of the catalytic domain of a human thioredoxin-like protein. European Journal of Biochemistry 2002;269:2060–8.
[43] Valko M, Rhodes CJ, Moncol J, Izakovic M, Mazur M. Free radicals, metals and antioxidants in oxidative stress-induced cancer. Chemico-biological Interactions 2006;160:1–40.
[44] Maulik N, Das DK. Emerging potential of thioredoxin and thioredoxin interacting proteins in various disease conditions. Biochimica et Biophysica Acta (BBA) – General Subjects 2008;1780:1368–82.
[45] Ren Q, Zhang RR, Zhao XF, Wang JX. A thioredoxin response to the WSSV challenge on the Chinese white shrimp, *Fenneropenaeus chinensis*. Comparative Biochemistry and Physiology Toxicology & Pharmacology: CBP 2010;151: 92–8.
[46] Mu C, Zhao J, Wang L, Song L, Song X, Zhang H, et al. A thioredoxin with antioxidant activity identified from *Eriocheir sinensis*. Fish & Shellfish Immunology 2009;26:716–23.
[47] Samoilov MO, Rybnikova EA, Tjulkova EI, Spyrou G, Pelto-Huikko M. The mitochondrial antioxidants thioredoxin-2 and Mn-superoxide dismutase are involved in the mechanisms of brain hypoxic tolerance. Doklady Biological Sciences: Proceedings of the Academy of Sciences of the USSR, Biological Sciences Sections/Translated from Russian 2002;387:498–500.
[48] Zhang Q, Li F, Wang B, Zhang J, Liu Y, Zhou Q, et al. The mitochondrial manganese superoxide dismutase gene in Chinese shrimp *Fenneropenaeus chinensis*: cloning, distribution and expression. Developmental & Comparative Immunology 2007;31:429–40.
[49] Bao Y, Li L, Zhang G. The manganese superoxide dismutase gene in bay scallop *Argopecten irradians*: cloning, 3D modelling and mRNA expression. Fish & Shellfish Immunology 2008;25:425–32.
[50] Segal AW. How neutrophils kill microbes. Annual Review of Immunology 2005;23:197–223.
[51] Aispuro-Hernandez E, Garcia-Orozco KD, Muhlia-Almazan A, Del-Toro-Sanchez L, Robles-Sanchez RM, Hernandez J, et al. Shrimp thioredoxin is a potent antioxidant protein. Comparative Biochemistry and Physiology Toxicology & Pharmacology: CBP 2008;148:94–9.
[52] Huang DJ, Chen HJ, Hou WC, Lin CD, Lin YH. Active recombinant thioredoxin h protein with antioxidant activities from sweet potato (Ipomoea batatas [L.] Lam Tainong 57) storage roots. Journal of Agricultural and Food Chemistry 2004;52:4720–4.